Some Approximations for the Dynamics of Spacecraft Tethers

A. H. von Flotow*
Massachusetts Institute of Technology, Cambridge, Massachusetts

This paper attempts a critical discussion of selected physical effects in the dynamics of spacecraft tethers, pointing out that for many purposes the simplest models are adequate. Spectral separation is invoked to decouple the motion into a slow libration akin to that of a rigid body upon which fast oscillations involving tether deformation and end-body attitude motions are superimposed. The effect of a slight quasiequilibrium tether curvature on this fast motion is illuminated via a linearized analysis.

Introduction

PAST analyses of the dynamics of spacecraft tethers have generally been of two types: either quite simple models were used, typically with the tether assumed to be straight and inextensible, or comprehensive simulations[1-3] were prepared for computer implementation. General agreement on the importance of various physical effects does not seem to have been reached. Each analyst has individually made the choice of which effects to model, sometimes quite arbitrarily. Reference 2 is a broad summary of work published to date, and includes 97 citations.

The work reported in this paper was motivated by the philosophy that the appropriate approach to developing an engineering model of a physical system is to include no more than the bare minimum of effects required to reproduce the behavior of interest. Since this is necessarily an iterative procedure, this paper builds upon insights gleaned from the results of previous analyses. Spectral separation is invoked to reduce the dynamics to a relatively fast vibrational motion, decoupled from and superimposed upon the slow roll/yaw librations of the system. It is suggested (with experimental evidence) that, because of the low tensions experienced by spacecraft tethers, nonlinear extensional stress/strain behavior will be important.

Infinitesimal perturbations of the tether from its slowly varying quasiequilibrium are described by a system of linear partial differential equations, in which longitudinal and lateral motion are coupled by slight curvature of the equilibrium shape. These equations are nondimensionalized and investigated with respect to wave propagation, revealing that for wave lengths much smaller than equilibrium radius of curvature, lateral and longitudinal motions effectively decouple. Assumption of point-mass dynamics for the endbodies leads to an eigen-analysis which yields eigenfrequencies and shapes, the first few of which can be quite different from those of the classic cable approximation. Effects of tether stiffness, curvature, tension, length, retrieval rate, etc., are illuminated in terms of nondimensional parameters.

The intent of this paper is to provide simple conceptual models of the motion of tethered satellites, both to guide development of future simulations and to provide a basis against which to compare simulation results.

Received March 11, 1987; revision received July 28, 1987.

*Assistant Professor, Department of Aeronautics and Astronautics.

Appropriate Models of Tether Elasticity

To date, models of tether elasticity have ranged from that of an inextensible chain to that of a beam with nonsymmetric cross section and with torsional strain energy. It is easy to show that the "bending length," l_B, beyond which the effects of bending stiffness, EI, are negligible compared to those of tension, T, is given by $l_B \approx \sqrt{EI/T}$. With tether diameter on the order of one millimeter, and tether tension on the order of a few Newtons, this bending characteristic length is on the order of a few centimeters. Thus, for such tethers, with lengths of many meters or kilometers, bending stiffness does not contribute significantly to global restoring forces, and a beam model is inappropriate.

Bending stiffness does, however, contribute nonlinearly to the extensional stress/strain behavior of such tethers. The natural form of a real wire is not straight. Residual stresses of unspecified origin and a spiral shape due to deployment from a reel will both be present. The characteristic length of these imperfections may very well be comparable to the bending length. Figure 1, adapted from Ref. 4, presents relevant experimental results.

Nonlinear Extensional Stiffness of a Wire

Spacecraft tethers will often operate under very low tension, even as low as a few Newtons for end masses of many hundreds of kilograms. We are thus interested in the extensional stress/strain behavior as tension approaches zero. The most common assumption has been bilinear; linear elastic for extensional strain and zero tension for compressive strain. The experimental results of Fig. 1, first reported in Ref. 4, show the behavior to be more complex.

Two approximate analyses of the force/deflection behavior of a wire with initial wrinkles can be offered. Both predict a similar nonlinear stress/strain behavior:

$$\varepsilon = -\left(\frac{\kappa}{T}\right)^2 + \frac{T}{EA} \tag{1}$$

(valid for small strain, approximately $-0.05 < \varepsilon < 0.01$). The strain ε is thus seen to be the sum of two contributions: a linear elastic extension proportional to the tension T and inversely proportional to the axial stiffness EA, and a nonlinear shortening due to the wire's tendency to return to its unstressed shape as $T \to 0$, The value of the constant κ depends upon the assumptions made in the derivations.

If an inextensible wire's unstressed shape is assumed to be a helix of radius r, pitch angle $\alpha \approx 0$, and arclength L (the wire is tightly wound on a reel of radius r), then the tension T required to extend the wire to a length h (while preventing untwisting)

is given by[5]

$$T=\frac{GJ}{r^2}\frac{h}{L}-\frac{EI}{r^2}\frac{h}{L}\left(1-\frac{1}{\sqrt{1-(h/L)^2}}\right) \qquad h<L \qquad (2)$$

where EI is the bending and GJ the torsional stiffness. If we define the strain with respect to the wire's arclength, $\varepsilon=(h-L)/L$, and limit $|\varepsilon|\ll 1$, then Eq. (2) reduces to

$$T=\frac{GJ}{r^2}-\frac{EI}{r^2}\frac{1}{\sqrt{-2\varepsilon}} \qquad \varepsilon<0 \qquad (3)$$

which, since $GJ\approx EI$ for isotropic materials and closed convex sections, becomes

$$\varepsilon\approx-\left(\frac{\kappa}{T}\right)^2 \qquad \kappa=EI/\sqrt{2}r^2 \qquad (4)$$

An alternative derivation attempts to model a slightly wrinkled unstressed shape by introduction of a sinusoidal planar wrinkle with amplitude Δ and wavelength Λ. It is not difficult to show that under this assumption, the tension/strain behavior of the axially inextensible wire becomes

$$\varepsilon=-\left(\frac{\kappa}{T}\right)^2 \qquad \kappa=32\sqrt{6}EI\Delta/\Lambda^3 \qquad (5)$$

as $h\to L$. Eq. (1) is then the sum of the nonlinear shortening of Eqs. (4) or (5), and the linear elastic extension T/EA.

The experimental points of Fig. 1 were measured for a length of Teflon-insulated stranded copper wire sold on a small plastic reel. This wire was under consideration for use as a spacecraft tether.[4] Plausible values have been inserted into Eqs. (1) and (4) to calculate the theoretical curve in Fig. 1.

It would be interesting to speculate about (or to measure) the low-tension stress/strain behavior of other candidate tethers. Effects of braiding, stranding, twist, and other tether details would potentially add nonlinearity to the nonlinearity introduced by residual stresses. The results summarized by Fig. 1 suggest that such nonlinear behavior will be much more important than many of the other nonlinear effects included in past analyses. For the mission studied in Ref. 4, the nonlinear flexibility, $1/\widetilde{EA}(\varepsilon)$, can be greater than the linear flexibility by a factor of up to one thousand.

In principle, it is possible to model this subtle effect of tether bending stiffness by using a beam model for the tether and resolving the details of the tether shape. The resolution demanded would be on the order of a few centimeters (the bending length) and would lead to a hopelessly large computer simulation for tethers several kilometers in length. The approached introduced in the preceding paragraphs would be to use an elastic cable model, with a nonlinear stress/strain behavior as in Eq. (1). Figure 2 indicates that the tether position would then be modeled to a precision on the order of the bending length, adequate for most purposes.

Reference Frames and Equations of Motion

The equations of motion of an elastic cable (no bending or torsional stiffness) have long been known[5] and are concisely expressed in vector notation

$$\mu\frac{\partial^2\boldsymbol{R}}{\partial t^2}=\frac{\partial}{\partial s}\left(T\frac{\partial\boldsymbol{R}}{\partial s}\right)+\boldsymbol{F} \qquad (6)$$

where μ is the mass per unit strained length of the tether and $\boldsymbol{R}(s,t)$ is the vector position of the tether as a function of time t and strained arclength s. Vector differentiation is performed in a Newtonian reference frame. The arclength is conveniently measured from one end of the tether, for example, within end body A. External forces per unit length are indicated by vector $\boldsymbol{F}$. The tension T is given as a function of ε, where $\varepsilon=\|\partial\boldsymbol{R}/s\|-1$, by Eq. (1). If the tether is to be modeled as constant length, Eq. (1) is replaced by the constraint $\|\partial\boldsymbol{R}/\partial s\|=1$. (The issue of when an inelastic model of the tether is appropriate is discussed in a subsequent section.)

The boundary conditions required to complete Eq. (6) will depend on the dynamics of the end bodies of the tethered satellite system. The force exerted by the tether on the end body A (at $s=s_A$) is just

$$\boldsymbol{F}_A=\left\{\left[T-\mu\left(\frac{\partial s_A}{\partial t}\right)^2\right]\frac{\partial\boldsymbol{R}}{\partial s}\right\}_{s=s_A} \qquad (7)$$

Note the appearance of the normally negligible thrusting term due to tether deployment.

Reference 3 reports the development of a simulation based upon a finite difference discretization of Eq. (6), boundary conditions built upon Eq. (7), and the assumption of suitable models for the endbodies. The reference frame chosen is Earth-centered inertial; thus, relative motion must be resolved as the small difference of two large numbers. In this reference frame, Eqs. (6) and (7) are highly nonlinear in the three components of $\boldsymbol{R}$.

A more common approach has been to introduce a tether reference frame[1,2] and to express tether motion with respect to

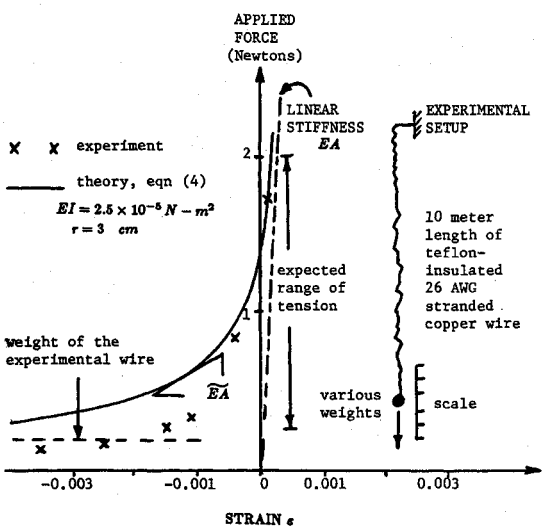

Fig. 1 A wire exhibits a nonlinear stress/strain relation due to straightening of initial wrinkles. This figure compares the results of one experiment with an analysis based upon the assumption that the wire is unstressed when wound on a spool of radius r.

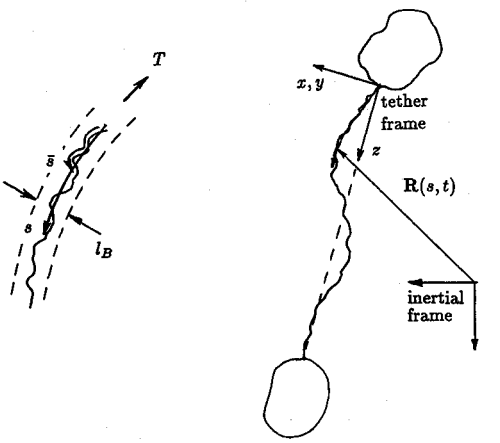

Fig. 2 It is proposed to forego detailed modeling of the tether "wrinkles" in favor of modeling only the approximate position and using a nonlinear stress/strain relation. The tether position would then be modeled with a resolution of approximately $l_B\approx\sqrt{EI/T}$.

this frame. This tether frame has historically been chosen with one axis defined by the tether attachment points on the two bodies and the other axes defined via their orientation with respect to the orbital plane (see Fig. 2). If tether deflections are expressed with respect to this frame, then the rotational motions of the reference frame add Coriolis, centripetal, and angular acceleration terms to the time derivatives of Eqs. (6) and (7), and the equations describing tether deflection are thus inertially coupled to those describing system attitude. Since the angular velocity of the tether reference frame is defined by endbody motion, which depends in part upon tether forces, the equations of motion governing system attitude are also coupled to the partial differential equations governing tether deflections.

The approach of Ref. 1, and many works cited in Ref 2, has been to simulate this system of equations numerically. The tether shape is discretized by the introduction of shape functions or by a lumped mass model. The resulting ordinary differential equations can then be integrated forward to time. Experience with these simulations has revealed the system to be "stiff"; some motions occur much faster than others, and the integration time step must be chosen to be a very small fraction of the orbital period.

The Approximation of Spectral Separation

An alternative approach to extracting information from a stiff system of ordinary differential equations is to introduce the approximation of spectral separation. This approximation is based upon the realization that the effect of coupling between fast and slow dynamics of a system is well approximated by the introduction of two assumptions:

1) The slow dynamics define a quasiequilibrium from the point of view of the fast dynamics.

2) The fast dynamics modify the slow dynamics quasistatically; that is, they participate in the slow dynamics at their instantaneous equilibrium levels.

The best reference for the theory and practice of spectral separation, with application to many examples, is perhaps an unpublished book draft.[6]

Table 1 is a summary of estimates of the eigenfrequencies of a tethered system, both in symbolic and numerical form.

Table 1 Estimates of periods of vibration of a tethered satellite system

Description	Symbolic	Numerical[a]
System pitch	$\frac{2\pi}{\sqrt{3}\omega_o}$	3100 s
System roll	$\frac{\pi}{\omega_o}$	2700 s
Elastic bounce	$2\pi\sqrt{\frac{Lm_Am_B}{EA(m_A+m_B)}}$	61 s[b]
Tether modes:		
first lateral	$2L\sqrt{\frac{\mu}{T}}$	440 s
first longitudinal	$2L\sqrt{\frac{\mu}{EA}}$	9 s[b]
End body attitude	$2\pi\sqrt{\frac{I_o}{Td}}$	Orbiter: 1000 s Subsatellite: 13 s

[a]Numerical values used are: orbital rate $\omega_o = 1.16 \times 10^{-3}$/s, (low earth orbit), axial stiffness $EA = 10^5$ N, Orbiter mass $m_A = 10^5$ kg, subsatellite mass $m_B = 500$ kg, tether length $L = 20$ km, tension $T = 40$ N, tether mass density $\mu = 5 \times 10^{-3}$ kg/m, Orbiter inertia $I_o = 10^7$ kg-m^2, Orbiter attach point offset $d = 10$ m, subsatellite inertia $I_o = 125$ kg-m^2, subsatellite attach point offset $d = 0.75$ m. [b]This period is based on a linear elastic model for tether axial stiffness. The nonlinear stress/strain behavior of the tether to be used for the Italian/American mission is not available.

The numbers used are representative of the Italian/American Shuttle tethered satellite system. Note that the numerical estimates for this specific system indicate that most internal motions will be much faster than the pitch and roll of the entire system. The one exception to this spectral separation is the pendular attitude oscillation of the Space Shuttle Orbiter due to tether tension acting at the end of the tether deployment boom.

The Quasiequilibrium Tether Shape

The attitude motion of a general rigid body in orbit, responding to environmental torques, is well understood.[7] The motion of a general flexible body in orbit, and its interaction with the gravitational field is less well understood. Initial studies have shown that the rigid body motion is essentially unperturbed by flexible deformations as long as these deformations remain small relative to system dimensions,[8] and their natural frequencies remain perhaps a factor of ten[9] larger than the orbital rate ω_o. Review of Table 1 reveals that, with the exception of Orbiter attitude motion, the natural frequencies of the internal motion of the tethered system are indeed much faster than orbital rate. If slow endbody attitude motion can be ignored or is actively controlled, the attitude librations of the tethered system will occur much like those of a rigid body, as long as internal deflections remain small compared to tether length.

References 10 and 11 have considered the equilibrium longitudinal strain and tension distributions in a tether, subject to the assumptions of linear elasticity and a constant gravitational gradient acting along the axis of a straight tether. These studies have mathematically confirmed the validity of a simple approximation, exact for infinitesimal tether strain. Tether tension is effectively constant if both end masses are much greater than tether mass, and spatially parabolic if tether mass is significant.

The quasiequilibrium shape of a tether is not necessarily straight. Lateral forces due to aerodynamic drag, gravity gradient, electrodynamic interaction with the Earth's magnetic field, and Coriolis effects due to retrieval or deployment of the tether from a massive end body will all deflect the tether laterally against tensile restoring forces. Each of these forces will vary with time and space, both in magnitude and direction, with much of the variation occurring at frequencies comparable to orbital rate. Order-of-magnitude estimates of these lateral forces are

Aerodynamic drag 10^{-6} to 10^{-5} N/m
(atmospheric density 10^{-14} to 10^{-13} g/cm^3)

Electrodynamic 2×10^{-5} N/m/A
(Earth's magnetic field in low earth orbit)

Gravity gradient $\upsilon \times 10^{-8}$ N/m
(υ is lateral deflection in meters)

Coriolis $\dot{L} \times 10^{-5}$ N/m
($\dot{L}$ is retrieval or deployment rate, in m/s)

Numerical values given in Table 1 have been used where needed.

The approximation of spectral separation permits calculation of an instantaneous tether shape by insisting upon static equilibrium with these slow lateral forces. If one assumes that the tether experiences an external force density $\boldsymbol{F}$, uniform in direction and magnitude along the wire, then the equilibrium curve is planar, and is given by the solution of

$$\frac{\partial}{\partial s}\left(T\frac{\partial \boldsymbol{R}}{\partial s}\right) + \boldsymbol{F} = 0 \tag{8}$$

together with an appropriate stress/strain relation. Since this curve will be very shallow, we will approximate it to be a portion of a circular arc of radius, R, $R \gg L$, and since the tether mass is much less than endbody mass, we will introduce the approximation that the equilibrium tension T is independent of s. Basic equilibrium analysis then yields $R = T/F_\perp$ ($F_\perp$ is the component of F perpendicular to the line connecting the tether attach points) and mid-point sag of $\delta = L^2/8R$. Using a tension of $T = 40$ N and an external force density of 2×10^{-5} N/m, yields a radius of curvature of $R = 2000$ km and a mid-point sag of $\delta = 25$ m for a tether length of 20 km. These values become $R = 200$ km, and $\delta = 2.5$ m for a tether length of 2 km and a tension of 4 N. The nondimensional equilibrium radius of curvature, $\bar{R} = R/L$, is thus seen to be very large (approximately 100) and independent of length.

References 8 and 9 define the libration of a flexible system in terms of the attitude of a reference frame, whose origin remains at the deformed system mass center, and whose attitude is defined by orthogonality of the system flexible and rigid body motion. The tether frame introduced in Fig. 2 satisfies this definition of attitude only approximately, even when the endbodies are modeled as point masses. Since the tether deflection from the straight condition is very small (approximately $1/2\ \bar{R}$), the curved tether will couple the two endbodies much as a straight tether would, and system libration is essentially the same as the libration of the tether frame. Reference 9 comes to a similar conclusion.

The slowly varying equilibrium shape we will consider can thus be summarized as follows: A global pitch and roll libration of the system creates a spatially near-uniform tension in the tether, which varies slowly in time. The equilibrium tether shape is nearly straight, with a shallow planar sag which slowly changes amplitude and swings about the line connecting the two tether attachment points. This equilibrium is static when observed on the time scales of internal tether modes.

Fast Tether Motions

Fast tether motions are of interest for several reasons:

1) Simulations have shown[2] that such tether motions may grow during retrieval.

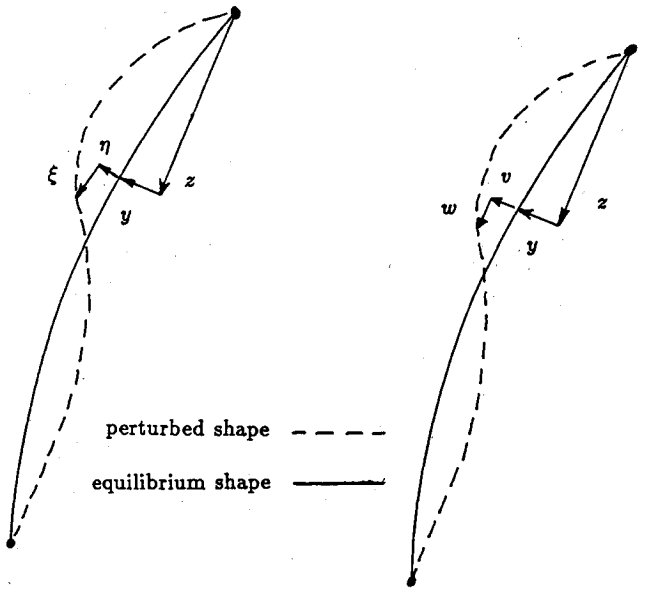

Fig. 3 The equations of motion governing infinitesimal tether deflections from the equilibrium curve can be expressed in several different coordinate systems. Curvilinear coordinates are useful for exposing the high-frequency wave-propagation limiting behavior and can be used for an eigenanalysis.

2) For maneuvers involving intermittent thrusting of the end bodies,[2,12] such fast tether motions will be excited directly.

3) The performance of kinetic isolation and subsatellite attitude control systems, based upon remote tethering of a sensitive payload to a noisy space station,[13] depends strongly on these tether dynamics.

Prior studies[14] of the dynamics of slightly curved elastic cables have concluded that even very slight equilibrium curvature can have a great influence upon perturbational motion. The fundamental symmetric mode of a pinned-pinned wire was shown to change character when a nondimensional parameter, $\lambda^2 = (L/R)^2 EA/T$, exceeded a critical value. The value of this parameter defines whether the tether behaves extensibly ($\lambda < 2\pi$) or inextensibly ($\lambda > 2\pi$) as it is perturbed from the equilibrium shape. The values of Table 1, together with the estimate of $R/L = 100$, yield a value of $\lambda = 2$, very near the critical value. Because these values are only estimates, and because the boundary conditions on spacecraft tethers are very different from those treated in Ref. 14, an analysis is appropriate.

This section derives the equations of motion governing infinitesimal perturbations of a slightly curved tether. The equilibrium curve is taken to be planar, and the perturbations are defined within this tether equilibrium plane, and normal to it. The effects of small inertial coupling due to the slow (order ω_o) angular velocities of the reference frame are ignored, consistent with the approximation of spectral separation.

Figure 3 defines the small perturbations $u(s, t)$, $v(s, t)$, $w(s, t)$, $\xi(s, t)$, and $\eta(s, t)$, of the tether with respect to its equilibrium shape, defined by $z(s)$ and $y(s)$ where s is the equilibrium arclength. This equilibrium arclength differs slightly from the natural arclength $\bar{s}$ (see Figure 2), depending upon the equilibrium tension. The tension is taken to be the sum of the equilibrium value $T(s)$ and a perturbation $\tau(s, t)$. Under the assumptions justified in the preceding paragraphs, and using the equilibrium defined by equation (8), Eq. (6) can be expanded to

In plane of tether equilibrium:

Axial

$$\frac{\partial}{\partial s}\left(T\frac{\partial w}{\partial s} + \tau\frac{\mathrm{d}z}{\mathrm{d}s}\right) = \mu\ddot{w} \tag{9}$$

Lateral

$$\frac{\partial}{\partial s}\left(T\frac{\partial v}{\partial s} + \tau\frac{\mathrm{d}y}{\mathrm{d}s}\right) = \mu\ddot{v} \tag{10}$$

Normal to the plane of tether equilibrium:

$$\frac{\partial}{\partial s}\left(T\frac{\partial u}{\partial s}\right) = \mu\ddot{u} \tag{11}$$

where terms of second and higher order in perturbational quantities have been dropped. The perturbational tension is given by

$$\tau = \widetilde{EA}\left(\frac{\mathrm{d}z}{\mathrm{d}s}\frac{\partial w}{\partial s} + \frac{\mathrm{d}y}{\mathrm{d}s}\frac{\partial v}{\partial s}\right) \tag{12}$$

where $\widetilde{EA}$ is the effective extensional stiffness of the tether at the equilibrium strain (see Fig. 1).

Reference 14 makes further approximations, valid for very shallow pinned-pinned catenaries, to manipulate Eqs. (9), (10), and (12) into a single second order partial differential for $v(s, t)$. We prefer the approach of Ref. 15, in which cable deflections are expressed in terms of components tangential and perpendicular to the equilibrium curve (see Fig. 3). Equations (9),

(10), and (12) can be transformed, using the transformation

$$w = \xi \frac{dz}{ds} - \eta \frac{dy}{ds} \tag{13}$$

$$v = \xi \frac{dy}{ds} + \eta \frac{dz}{ds} \tag{14}$$

into an equivalent system.

In plane of tether equilibrium:

Parallel to equilibrium tether

$$\frac{\partial}{\partial s}\left(\widetilde{EA}\frac{\partial \xi}{\partial s}\right) - \left(\mu \frac{\partial^2 \xi}{\partial t^2}\right) = -\frac{T}{R}\left(\frac{\partial \eta}{\partial s} - \xi \frac{1}{R}\right) - \frac{\partial}{\partial s}\left(\frac{\widetilde{EA}}{R}\eta\right) \tag{15}$$

Perpendicular to equilibrium tether

$$\frac{\partial}{\partial s}\left(T\frac{\partial \eta}{\partial s}\right) - \left(\mu \frac{\partial^2 \eta}{\partial t^2}\right) = \frac{\widetilde{EA}}{R}\left(\frac{\partial \xi}{\partial s} + \eta \frac{1}{R}\right) + \frac{\partial}{\partial s}\left(\frac{T}{R}\xi\right) \tag{16}$$

where $R = (dy/ds\,d^2x/ds^2 - dx/ds\,d^2y/ds^2)^{-1}$ is the equilibrium radius of curvature of the tether. Equation (11) remains unchanged.

Equations (11), (15), and (16) now describe the perturbational motion of an elastic cable from its planar equilibrium curve. The curve need not be shallow, nor need the radius of curvature R be constant with s. It is clear that curvature couples the two components of the planar motions; Eqs. (15) and (16) are coupled by terms involving $1/R$. As $R \to \infty$, the coupling disappears, and the equations are reduced to the familiar decoupled wave equations for axial and lateral motion of an elastic cable. Motion normal to the equilibrium plane remains unaffected by curvature.

Wave Propagation Along the Tether

Equations (16) and (17) are suitable for investigation of the intuition that high frequency tether motion is effectively described by propagation of decoupled lateral and tangential waves. We assume a solution of the form

$$\begin{pmatrix} \xi \\ \eta \end{pmatrix} = \begin{pmatrix} \xi_o \\ \eta_o \end{pmatrix} e^{\gamma(\omega,s)s + i\omega t} \tag{17}$$

where $\gamma(\omega,s) = \alpha(\omega,s) + ik(\omega,s)$ is known as the propagation coefficient. Substitution of Eq. (17) into Eqs. (15) and (16) yields a pair of coupled second order polynomials in γ and ω. These polynomials are satisfied along the lines sketched in Fig. 4. We see that wave propagation becomes nondispersive for $kR \gg 1$, that is, when the wavelength becomes small relative to the radius of curvature. Since the frequency has been nondimensionalized with respect to lateral wave speed, $\sqrt{T/\mu}$, three values of $T/\widetilde{EA}$ (assumed constant with s) give three different values of nondimensional tangential wave speed. Investigation of the corresponding wave-mode eigenvector, $(\xi_o,\eta_o)^T$, reveals that the response consists of pure extensional $(\xi_o,\eta_o) = (1, 0)$, or pure lateral $(\xi_o,\eta_o) = (0,1)$ motion for $kR \gg 1$. An order-of-magnitude analysis of the terms of Eqs. (16) and (17), as $|\gamma R| \to \infty$, will yield a similar insight.

Natural and Forced Motions of the Tethered System

Irvine and Caughey[14] report an approximate eigenanalysis of Eqs. (9), (10), and (12) for pinned-pinned boundary conditions and shallow parabolic catenaries. They conclude that the only mode strongly affected by slight curvature of an elastic cable is the first symmetric lateral mode. For analysis of a tethered spacecraft system, one is interested in different boundary conditions. A general endbody of such a tethered system can provide a complex boundary condition, including effects of endbody flexibility and attitude motion. This section

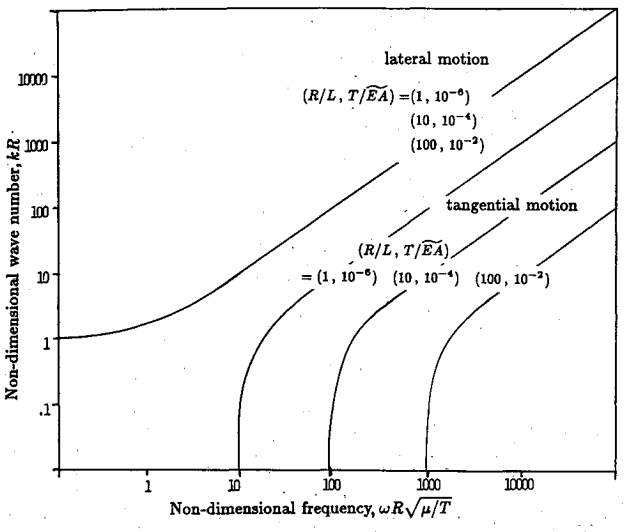

Fig. 4 Dispersion curves of lateral and tangential waves propagating along a tether with uniform equilibrium tension and radius of curvature.

formulates the eigenanalysis for arbitrary boundary conditions, and shows representative solutions for the simplest; one end is effectively pinned by attachment to a very massive body, the other end is connected to a point mass only several times more massive than the tether.

Introduction of the nondimensional cross sectional vector

$$\Gamma = \left(\xi/L, \widetilde{EA}/T\frac{\partial \xi}{\partial s}, \eta/L, \frac{\partial \eta}{\partial s}\right)^T \tag{18}$$

permits writing (Fourier transformed) Eqs. (15) and (16) as

$$\Gamma' = \begin{pmatrix} 0 & \epsilon & 0 & 0 \\ -\bar{\omega}^2 + 1/\bar{R}^2 & 0 & 0 & -1/\bar{R}\varepsilon \\ 0 & 0 & 0 & 1 \\ 0 & 1/\bar{R} & -\bar{\omega}^2 + 1/\bar{R}^2\varepsilon & 0 \end{pmatrix} \Gamma \tag{19}$$

where $\varepsilon = T/\widetilde{EA}$, $\bar{R} = R/L$, $\bar{\omega} = \omega L\sqrt{\mu/T}$, and the spatial derivative is taken with respect to a nondimensional distance, $\Gamma' = L\partial\Gamma/\partial s$.

Boundary conditions on either end of the tether are conveniently expressed as a matrix equation

$$\boldsymbol{B}(\bar{\omega})\Gamma = \boldsymbol{f} \tag{20a}$$

where $\boldsymbol{f}$ is the vector of applied forces or enforced displacements, as appropriate. To define a pinned end at $s = 0$ Eq. (20a) would employ

$$\boldsymbol{B} = \begin{pmatrix} 1 & 0 & 0 & 0 \\ 0 & 0 & 1 & 0 \end{pmatrix} \qquad \boldsymbol{f}_o = \begin{pmatrix} \xi/L \\ \eta/L \end{pmatrix}_{s=0} \tag{20b}$$

and $\boldsymbol{f}_o$ is an enforced nondimensional displacement. A point mass m at $s = L$ is described by

$$\boldsymbol{B} = \begin{pmatrix} -\dfrac{m}{\mu L}\bar{\omega}^2 & 1 & 0 & 0 \\ 0 & 0 & -\dfrac{m}{\mu L}\bar{\omega}^2 & 1 \end{pmatrix} \qquad \boldsymbol{f}_1 = \begin{pmatrix} f_\xi/T \\ f_\eta/T \end{pmatrix}_{s=L} \tag{20c}$$

where f_ξ and f_η are external forces applied to the point mass. The general form of the solution of Eq. (19) is

$$\Gamma(s,\bar{\omega}) = \begin{pmatrix} \Gamma_1 e^{\gamma_1 s/L} & \Gamma_2 e^{\gamma_2 s/L} & \Gamma_3 e^{\gamma_3 s/L} & \Gamma_4 e^{\gamma_4 s/L} \end{pmatrix} \begin{pmatrix} C_1 \\ C_2 \\ C_3 \\ C_4 \end{pmatrix} \tag{21}$$

where Γ_i is the ith eigenvector of the matrix in Eq. (19) and $\gamma_i(\bar{\omega})$ is the corresponding eigenvalue. Application of boundary conditions at the two ends, each in the form of Eq. (20a), permits evaluation of the constants C_i, $i = 1,2,3,4$ in terms of the force vector $(f_o, f_1)^T$. The response anywhere along the tether can then be expressed in terms of a matrix of transfer functions

$$\Gamma(s,\bar{\omega}) = \boldsymbol{H}(s,\bar{\omega}) \begin{pmatrix} f_o \\ f_1 \end{pmatrix} \tag{22}$$

These 16 transfer functions can be evaluated for any value of s, $0 < s < L$, and any value of $\bar{\omega}$, and relate the response along the tether to the excitation at the two ends.

Transfer Functions

The transfer functions of Eq. (22) will vary slowly with time because they depend upon the current equilibrium condition. This equilibrium establishes values of tension T and radius of curvature R, and defines the directions of ξ, η, and u. [Note that deflections normal to the plane of tether equilibrium u decouple from ξ and η. The relevant transfer functions can be derived from Eq. (11) and suitable boundary conditions.]

Figure 5 gives a plot of $H_{1,2}(L,\bar{\omega})$, parameterized with three nondimensional groups: $\bar{R} = R/L$, $\varepsilon = T/\widetilde{EA}$, and $m/\mu L$. This transfer function shows the tangential acceleration of the far end of the tether ($s = L$) being excited by a unit lateral acceleration at the near end ($s = 0$). If the equilibrium tether shape were straight, this response would be zero. Figure 5a shows, for a fixed equilibrium $T/\widetilde{EA}$ and a fixed subsatellite mass ratio $m/\mu L$, the ratio of $\xi(s = L)$ and $\eta(s = 0)$ is a function of frequency. As expected, the low frequency response tends toward zero as the tether becomes straight, $R/L \to \infty$. It is clear that even slight tether curvature will couple these two motions, particularly at resonance. Figure 5b shows the same curves for an increased value of $T/\widetilde{EA}$. The low frequency limiting behavior remains unchanged; however, the nondimensional frequencies of the first few resonances are strongly affected.

Such transfer functions are of prime importance to designers of tether based vibration isolation systems, and even more to those contemplating attitude control of a tethered subsatellite. One such design[13] has been based upon the assumption that tether dynamics are those of a massless, straight, viscoelastic spring. The axis crosscoupling of Fig. 5 may have a major effect on the performance and stability of such an attitude control scheme.

Tether Modes

Figures 5a and 5b yield little insight into the character of the underlying vibration. Figure 6 shows the evolution of the first few natural frequencies and mode shapes as a function of two nondimensional parameters, R/L and $T/\widetilde{EA}$. R/L is held fixed at two values, $R/L = 10$, 100, whereas $T/\widetilde{EA}$ is varied. Strong coupling is predicted between pendular motion and lateral tether deflection whenever $\lambda^2 > 10$. At $\lambda^2 \approx 30$ (very close to the value predicted by Ref. 14 for fixed boundary conditions) the two lowest mode shapes become identical, and their contribution disappears from all transfer functions. A root locus of these poles of the model in the vicinity of $\lambda^2 = 30$ shows the two frequencies coalescing at $\lambda^2 = 32$, and becoming complex for greater values of λ^2. The implied instability, oscillatory with frequency, $\bar{\omega} = 2.5$, is not understood and is suspected to be of mathematical rather than physical origin. The boundary value problem defined by partial differential equations (15) and (16)

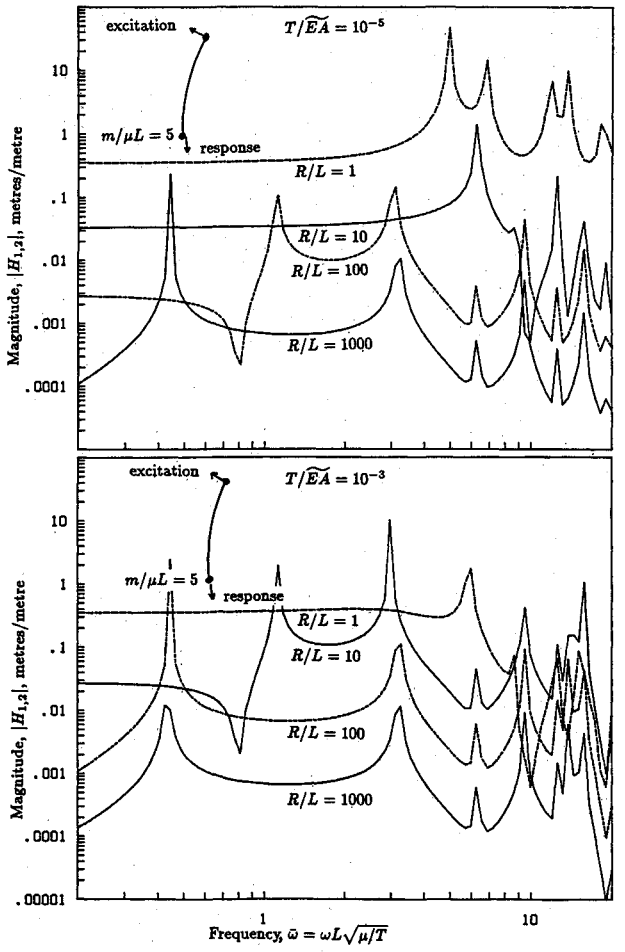

Fig. 5 Transfer functions of the tangential response at one end of the tether to a lateral excitation at the other end.

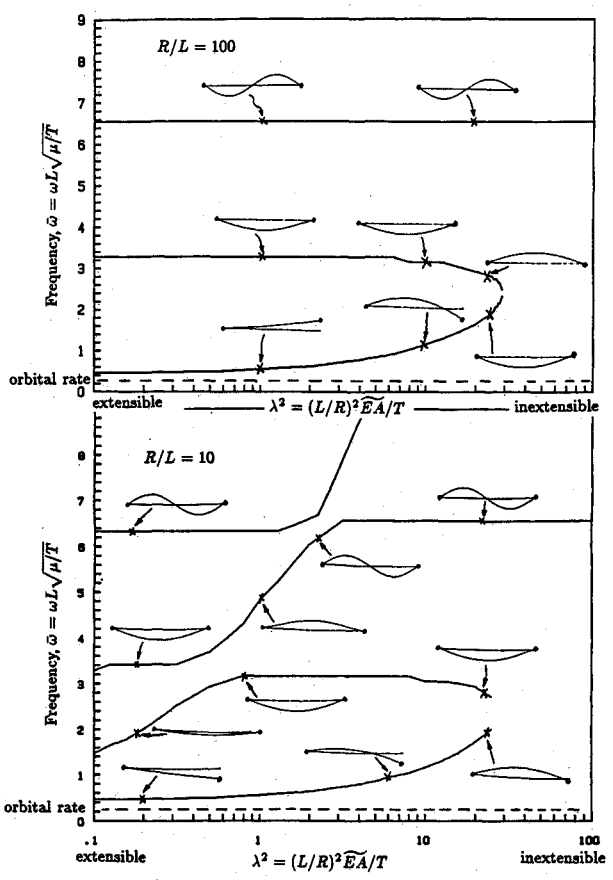

Fig. 6 Trends of the first few natural frequencies and mode shapes of a tethered system with slight equilibrium curvature. One end mass is effectively infinite, the other has five times the tether mass, $m/\mu L = 5$.

and the boundary conditions [Eq. (20a)] can be shown to be self-adjoint. Explanation of this unexpected instability remains a mystery. Lateral and longitudinal motion can also couple strongly. Figure 6b shows such coupling between the first few lateral modes and the longitudinal bounce mode. Tether curvature, even as low as $R/L = 100$, can greatly modify the behavior.

Effect of Deployment or Retrieval

The preceding analysis has ignored effects of deployment and retrieval on the fast tether dynamics, both the Coriolis coupling due to a tangential velocity of the tether and the gradual length change.

Effect of Tether Translational Velocity

Retrieval of the tether to a massive end body will result in a translational velocity of the tether along its equilibrium curve. This translational velocity will add Coriolis coupling terms to Eqs. (15) and (16). Reference 16 has shown that such translational velocity will have a negligible effect upon the perturbational motion of an elastic catenary as long as this velocity is much less than the classic lateral wave speed $\sqrt{T/\mu}$. Retrieval speed of spacecraft tethers is limited by attitude stability considerations to $\dot{L}/L \ll \omega_o$, which, on the basis of the spectral separation assumed, implies $\dot{L} \ll \sqrt{T/\mu}$. Ignoring the effect of this Coriolis coupling is thus consistent with the assumption of spectral separation upon which the preceding analysis is based.

Effect of Gradual Length Changes

The preceding paragraph argues that relative tether length changes will be small over the period of even the fundamental tether mode. When this is satisfied, tether mode shapes will be effectively those of the constant length system, but their amplitude will vary slowly with the length. An approximate expression for this dependence can be derived by assuming a given mode shape, of amplitude a and geometrically independent of length, and insisting upon conservation of strain energy. This leads to the conclusion that $\widetilde{EA}a^2/L$ remains constant if the mode is primarily tangential and that Ta^2/L remains constant if the mode is primarily lateral. Since T is approximately proportional to length, lateral deflection amplitudes should be approximately independent of length. This agrees with the simulation results reported in Ref 2. The dependence of $\widetilde{EA}$ on length is more difficult to approximate. If the nonlinear effects of Fig. 1 can be neglected, then $\widetilde{EA} = EA$ is independent of length, and tangential tether vibrations should decrease during retrieval according to $a \sim \sqrt{L}$. If the tether mode is coupled lateral and axial, then its dependence on length should be some weighted average of the individual dependencies.

Modeling Limitations

The insights gained in these analyses were achieved only at the cost of rather severe assumptions. Interest was restricted to tethered systems involving one tether and two endbodies, with a spectrum permitting the approximation of spectral separation. The results of Figs. 5 and 6 show that for some choices of parameters, the assumption of spectral separation will be violated. The conclusions reached will not be applicable to very different systems such as tethers with negligible end masses, massive, tapered tethers, multiple tethers, rapidly spinning tethers, and many others.

The eigenanalysis presented is based upon the assumption of small deflections. References 17 and 18 have considered larger amplitude motion of cables. Reference 17 shows that the quadratic terms in the strain energy expression of a shallow catenary remain dominant only as long as deflections remain small compared to the equilibrium sag. Equations (15) and (16) are thus only valid for very small deflections, less than $\delta = L/8\bar{R} \approx 0.001L$. Reference 18 derives the equations of motion of a sequence of assumed deflection modes of a spacecraft tether, where the reference state is taken to be straight and axially unstrained. This work shows that nonlinear effects will couple axial and both directions of lateral deflection, and by integration of the equations of motion shows this coupling to be significant when deflections become as large as $0.1L$.

Unmodeled effects that threaten to be important are endbody attitude motion and flexibility. Very slow endbody attitude motion would still permit spectral separation, simply redefining the reference equilibrium. Fast endbody attitude motion and endbody flexibility will potentially couple strongly to the tether modes. Table 1 estimates the subsatellite pendular motion to have a period of 13 s. One should expect strong coupling of this motion with the bounce mode and with several (perhaps the 40th) lateral tether modes. The introduction of fast endbody attitude dynamics would require the use of at least two more nondimensional parameters, perhaps d/L and $d\sqrt{m/I_o}$, where d is the offset between the tether attach point and the endbody mass center, m its mass, and I_o its inertia. A study of the effects of this coupling is left as a topic of future research.

Summary

This paper has investigated the dynamics of typical tethered spacecraft systems. The motion is shown to occur at two time scales, one comparable to orbital rate, the other much faster. Spectral separation is invoked to approximately decouple this motion. Fast tether vibrations occur with respect to a slowly varying quasi-equilibrium. The equilibrium shape of the tether is estimated to be slightly sagged from a straight line, and the small perturbations from this equilibrium are described by a system of linear partial differential equations. Nondimensional parameter groups are identified which govern the character of the fast tether vibrations.

Acknowledgments

The work summarized by this paper was begun during the summer of 1986 during a research visit at the German Aerospace Research Establishment, DFVLR Oberpfaffenhofen. The visit was made possible by the hospitality of the DFVLR, in particular Dr. Konrad Reinel, and by the generosity of the Alexander von Humboldt Foundation. The work was continued at the Massachusetts Institute of Technology under the sponsorship of the U.S. Air Force Office of Scientific Research with Dr. Anthony Amos as monitor. Computations were performed by Jeff Morse as part of MIT's Undergraduate Research Opportunities Program.

References

[1]Lang, D., *TOSS (Tethered Object System Simulation) Reference Manual,* Version C, May 1985; private communication, Jan. 1986.

[2]Misra, A. K. and Modi, V. J., "A Survey on the Dynamics and Control of Tethered Satellite Systems," AAS Paper 86-246, Sept. 1986; also, *Advances in Astronautical Sciences,* Vol. 62, 1987.

[3]Kohler, P., Maag, W., Wehrli R., Weber, R., and Brauchli, H., "Dynamics of a System of two Satellites Connected by a Deployable and Extensible Tether of Finite Mass," Vols. 1 and 2, ESA CR Contract 2992/76/NL/AK(SC), Oct. 1978.

[4]von Flotow, A. H. and Williamson, P. R., "Deployment of a Tethered Plasma Diagnostics Satellite into Low Earth Orbit," *Journal of the Astronautical Sciences,* Vol. 34, Jan-March 1986, p. 65.

[5]Love, A. E. H., *A Treatise on the Mathematical Theory of Elasiticity*, Dover, 1944.

[6]Bryson, A. E., *Control of Spacecraft and Aircraft*, Stanford University Lecture Notes, Sept. 1985.

[7]Hughes, P. C., *Spacecraft Attitude Dynamics*, Wiley, New York, 1986.

[8]Diarra, C. M. and Bainum, P. M., "On the Accuracy of Modeling the Dynamics of Large Space Structures," *Proceedings of IAF'85, 36th Congress of the International Astronautical Federation*, Stockholm, Sweden, October 1985.

[9]Ashley, H., "Observations on the Dynamic Behaviour of Large Flexible Bodies in Orbit," *AIAA Journal*, Vol. 5, March 1967, pp. 460–469.

[10]Storch, J. and Gates, S., "The Dynamics of a Uniform Tether with a Tip Mass Subject to Gravitational Body Forces," Charles Stark Draper Lab. CSDL-R1791, Internal Rept. Cambridge, MA, June 1985.

[11]Misra, A. K. and Modi, V. J., "Frequencies of Longitudinal Oscillations of Tethered Satellite Systems," AIAA Paper 86-2274, Aug. 1986.

[12]Xu, D. M., Misra, A. K., and Modi, V. J., "Thruster Augmented Active Control of a Tethered Subsatellite System During its Retrieval," *Journal of Guidance, Control, and Dynamics,* Vol. 9, Nov.-Dec. 1986, pp. 663–672.

[13]Lemke, L. G., Powell, J. D., and He, X., "Attitude Control of Tethered Spacecraft," *Journal of the Astronautical Sciences,* Vol. 35, Jan.-March 1987, pp. 41–56.

[14]Irvine, H. M. and Caughey, T. K., "The Linear Theory of the Free Vibration of a Suspended Cable," *Proceedings of the Royal Society of London,* A. 341, London, 1974, pp. 299–315.

[15]Saxon, D. S. and Cahn, A. S., "Modes of Vibration of a Suspended Chain," *Quarterly Journal of Mechanics and Applied Mathematics,* Vol. VI, Pt. 3, 1953, pp. 273–285.

[16]Simpson, A., "On the Oscillating Motions of Translating Elastic Cables," *Journal of Sound and Vibration,* Vol. 20, 1972, pp. 177–189.

[17]Hagedorn, P. and Schäfer, B., "On Non-Linear Vibrations of an Elastic Cable," *International Journal of Non-Linear Mechanics,* Vol. 15, 1980, pp. 333–340.

[18]Misra, A. K., Xu, D. M., and Modi, V. J., "On Vibrations of Orbiting Tethers," *Acta Astronautica,* Vol. 13, No. 10, 1986, pp. 587–597.